

## Dependence of some plasma parameters on $ap$ in a dc helium hollow cathode discharge

O.H. Chin and C.S. Wong

*Plasma Research Laboratory, Physics Department, University of Malaya, 50603 Kuala Lumpur, Malaysia*

(Received 16 September 2001)

The dependence of the electron temperature, electron density and plasma potential of a dc helium hollow cathode discharge with the product of the hollow cathode diameter and gas pressure  $ap$  is investigated. These are then compared with reported works and correlated to the optimum pressure range in which the hollow cathode effect is said to be fully developed.

**Keywords:** Electron density; electron temperature; plasma potential; two-temperature

### I. INTRODUCTION

Much study has been made on the hollow cathode discharge since it was first reported by Paschen [1]. Although the hollow cathode may take many forms, the following operating conditions are generally applicable [2,3]:

- (1)  $1 \text{ torr-cm} < ap < 10 \text{ torr-cm}$  for rare gases ( $a$  being the diameter and  $p$  the gas pressure;  $a > 2 \times$  cathode dark space width  $d_k$ );
  - (2) ratio of cathode length to diameter  $\ell:a \leq 7$ ;
- provided that the negative glow is confined within the hollow cathode cavity and the hollow cathode structure is not embedded within another.

The widely accepted definition of the hollow cathode effect is the enhanced emission from the negative glow within the cathode cavity as well as the increase in discharge current density, up to several orders of magnitude at constant potential resulting from the cathode geometry [4,5]. Optimum mode of hollow cathode effect has been identified on basis of fraction of fast electrons in the glow being at maximum [6]. However, Kirichenko et al. [7] defined an optimum pressure range for fully developed hollow cathode discharge in which cathode fall potential increases with pressure at fixed current.

Mechanisms believed to be responsible for the hollow cathode effect are primarily due to its efficient confinement of particles (neutrals, ions, electrons) due to its geometry [4,8-14]. These mechanisms depend on a number of parameters such as  $p$ , discharge current  $I$  and voltage  $V$ , hollow cathode geometry and material, and filling gas. It is difficult to identify which of these mechanisms is the dominant one (if indeed there is one). It is inherent of gas discharges to have any of its chosen property to depend on a number of others. Thus the necessity to simplify into invariant groups of parameters as in the similarity laws [15], one of which is the product of the gas pressure and cathode dark space width  $pd_k$ .

However, the product  $ap$  is more appropriate and widely used in the hollow cathode discharge, and reasonable compliance to similarity law can still be achieved.

This work aims to correlate and compare some of the plasma parameters of the hollow cathode discharge in relation to the product  $ap$  obtained in a dc hollow cathode arrangement operated with helium filling gas. Comparison with reported works [16-17] using different hollow cathode arrangement is also made.

### II. EXPERIMENTAL SETUP AND ARRANGEMENT

The schematic of the hollow cathode arrangement is shown in Fig. 1. The stainless steel hollow cathode is interchangeable and two different hollow cathodes of diameters 6.5 mm (HC6512) and 16mm (HC1612) with fixed length 12 mm are used. The anode is a hollow cylinder with inner diameter 13 mm and the interelectrode separation is fixed at 9.5 mm.

The swept single Langmuir probe technique is used to determine the electron temperature and density. The probe is inserted into the hollow cathode tube as shown in Fig. 2. The probe current is measured across the 1 k $\Omega$  resistor via a lowpass filter model *Stanford Research* SR 650 while the probe voltage  $V_p$  is taken across the output of the voltage sweep amplifier with respect to the dc bias potential  $V_B$ . From these, the electron temperature  $T_e$ , electron density  $n_e$ , and plasma potential  $\phi_s$  are determined. In cases where two distinct linear regions are obtained on the electron retardation region in the plot of  $\ln(I_e)$  against  $V_p$ , it is interpreted as evidence of two groups of electrons with Maxwellian distributions at different temperatures,  $T_s$  (slow) and  $T_f$  (fast). The procedure to evaluate the temperatures and densities of the two groups of electrons are given by Tkachenko and Tyutyunnik [16]. The average electron energy  $T_e$  and total electron density  $n_e$  are then estimated according to

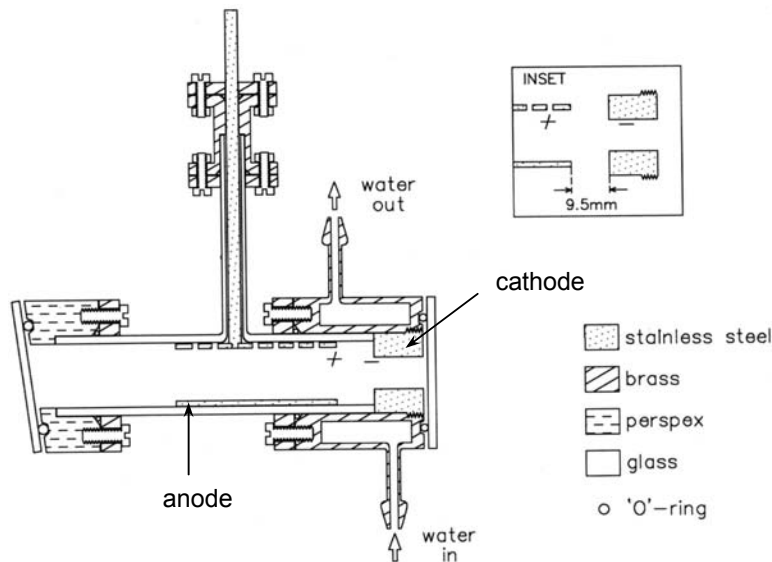


FIG. 1. Schematic of the water-cooled hollow cathode discharge tube arrangement. Inset shows the cathode-anode separation.

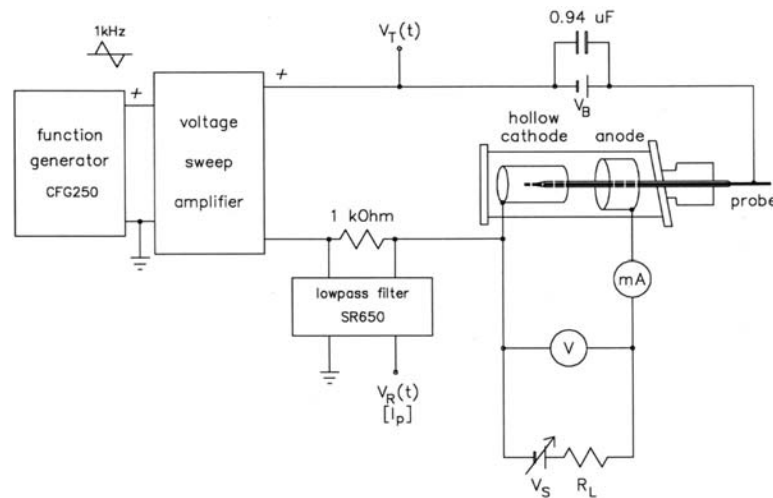


FIG. 2. Schematic of the hollow cathode discharge and the swept single Langmuir probe circuits.

$$n_e T_e = n_s T_s + n_f T_f \quad (1)$$

$$\text{and } n_e = n_s + n_f \quad (2)$$

### III. RESULTS AND DISCUSSION

It is more appropriate to study the behaviour of the plasma parameters with respect to the product of the hollow cathode diameter and operating pressure  $ap$  (in cm-torr) as it can be related to the optimum pressure regime where the hollow cathode discharge is said to be fully developed. Thus the dependence of the electron temperatures and densities measured at the axis and side

of the hollow cathode is shown in Figs. 3 – 7. Those measured at the side are shown for the case of HC6512 only at 2 mm off-axis. The corresponding variation of the discharge voltage  $V_A$  and plasma potential  $\phi_s$  with  $ap$  at fixed discharge current  $I_A$  of 40 mA is shown in Fig. 8; from which the optimum pressure range is estimated at  $ap = 3 - 6$  cm-torr for HC6512. This is well within the operating conditions for a hollow cathode discharges stated earlier. In the case of HC1612, there is insufficient data points to determine the optimum pressure range. The trend of the variation of the plasma potential  $\phi_s$  follows that of the discharge voltage  $V_A$  except that it is at lower value; the difference ranging from 4 V to 48 V.

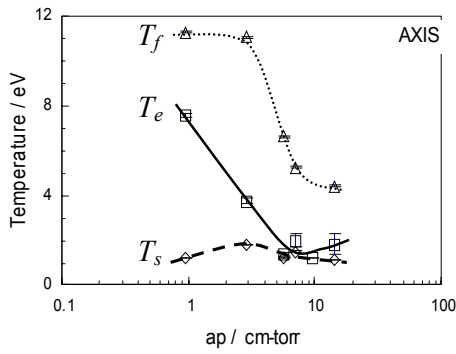


**FIG. 3.** Variation of electron temperatures with  $ap$  at the axis of the hollow cathode cavity with  $I_A = 40$  mA

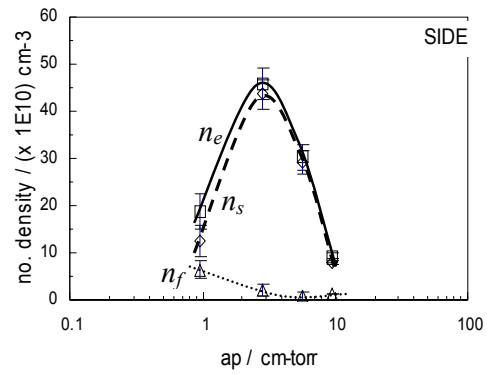


**FIG. 6.** Variation of electron densities with  $ap$  at the side of the hollow cathode cavity with  $I_A = 40$  mA.

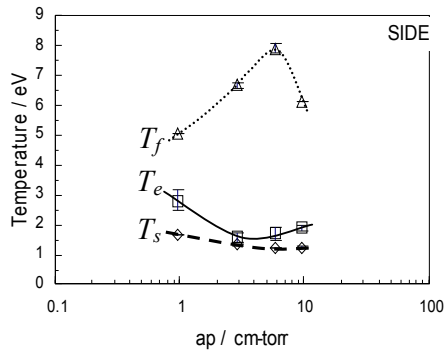


**FIG. 4.** Variation of electron temperatures with  $ap$  at the side of the hollow cathode cavity with  $I_A = 40$  mA

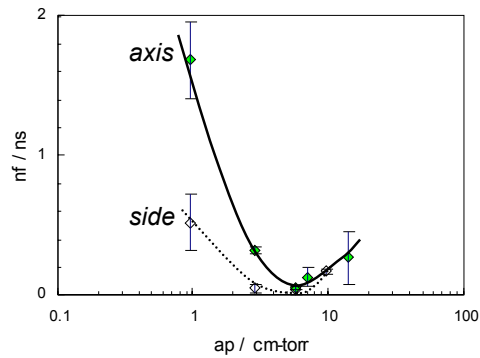


**FIG. 7.** Variation of the ratio of fast to slow electron densities  $n_f / n_s$  with  $ap$  at fixed  $I_A = 40$  mA.

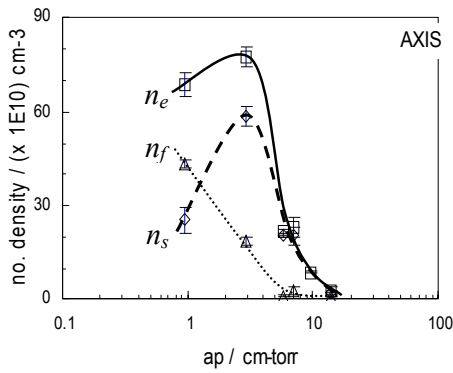


**FIG. 5.** Variation of electron densities with  $ap$  at the axis of the hollow cathode cavity with  $I_A = 40$  mA

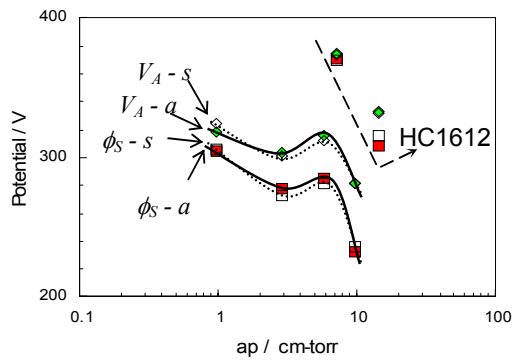


**FIG. 8.** Variation of the discharge voltage  $V_A$  and plasma potential  $\phi_s$  with  $ap$ .  
 $a$  : axis;  $s$  : side

At the axes of the hollow cathodes (Fig. 3), the average electron temperature  $T_e$  falls as  $ap$  is increased with a minimum of 1.2 eV at approximately 7 cm-torr.

The temperature of the slow electrons  $T_s$  (ranges from 1.1 – 1.8 eV) varies little with  $ap$  though a slight peak of 1.8 eV is observed at 3 cm-torr. The fast electrons,

however, manifest almost constant temperature  $T_f$  of 11.3 eV until 3 cm-torr before falling as  $ap$  is further increased. The temperatures at the side are shown only for the HC6512.  $T_e$  at the side (shown in Fig. 4 for the hollow cathode HC6512 only) falls gently with increasing  $ap$  until 1.6 eV at approximately 3 cm-torr, after which it rises instead.  $T_s$  also falls gently from 1.7 eV to 1.2 eV with increasing  $ap$ . However,  $T_f$  increases with  $ap$  initially until 7.9 eV at 6 cm-torr before decreasing.

The total electron density  $n_e$  and the density of the slow electrons  $n_s$  rise with increasing  $ap$  until 3 cm-torr ( $n_e = 78 \times 10^{10} \text{ cm}^{-3}$  and  $n_s = 59 \times 10^{10} \text{ cm}^{-3}$ ), before falling on further increase of  $ap$  (Fig. 5). Similar trends are observed for variation of  $n_e$  and  $n_s$  at the side of the hollow cathode cavity (Fig. 6), peaking at  $ap \cong 3$  cm-torr with  $n_e = 46 \times 10^{10} \text{ cm}^{-3}$  and  $n_s = 44 \times 10^{10} \text{ cm}^{-3}$ . The density of fast electrons  $n_f$  at the axis of the hollow cathode, however, falls steeply initially until  $0.6 \times 10^{10} \text{ cm}^{-3}$  at  $ap \cong 6$  cm-torr, after which it is almost constant. The initial fall of  $n_f$  measured at the side of HC6512 is gentler from  $6.6 \times 10^{10} \text{ cm}^{-3}$  to  $1.2 \times 10^{10} \text{ cm}^{-3}$  at  $ap \cong 6$  cm-torr, after which it increases slightly. The occurrence of the peaks in  $n_e$  and  $n_s$  seems to correspond to the lower limit of the optimum pressure range while the minimum of  $n_f$  corresponds to the upper limit of the same range.

The ratio of the number of fast electrons to the slow ones  $n_f/n_s$  shown in Fig. 7 falls with increasing  $ap$  until 6 cm-torr before rising slightly with further increase of  $ap$ . In relation to the optimum pressure range (Fig. 8), this minimum corresponds to the upper limit of the range. This ratio is higher at the axis than at the side until  $ap = 6$  cm-torr. Beyond the optimum pressure range, this ratio measured at the axis and side is almost the same. Thus it can be said that the number of fast electrons with respect to the number of slow electrons is higher at the axis than at the side in a fully developed hollow cathode discharge.

These variation of plasma parameters with  $ap$  are compared to those obtained from reported works by Tkachenko and Tyutyunnik [16] and Howorka and Pahl [17]. The dependence of the various plasma parameters discussed above on the product  $ap$  deduced from references [16] and [17] are shown in Figs. 9a – 9d and 10a – 10d respectively. These parameters are measured at the axes of their hollow cathode discharge configuration. Table I gives a summary of the various configurations of the hollow cathode discharge systems compared.

Reference [17] shows the lowest electron temperatures, the highest value being halved those in the other two systems. The dependence of  $T_e$  on  $ap$  shown by the three different systems are similar with their respective minima occurring at slightly beyond the upper limit of the optimum pressure range. The trend of

variation of  $T_s$  and  $T_f$  with  $ap$  differs for the three systems. The variation of  $T_s$  in reference [16] is similar to its  $T_e$  while  $T_s$  from reference [17] decreases with increasing  $ap$ .  $T_f$  from reference [16] peak at  $ap = 1.2$  cm-torr before decreasing with further increase in  $ap$  while  $T_f$  from reference [17] mimics its  $T_e$  dependence.

The magnitude of the electron densities varies with the different systems by about one order of magnitude; lowest in reference [16] and highest in the present system. The trends of the electron densities  $n_e$ ,  $n_s$  and  $n_f$  with  $ap$  are generally similar in the three systems; though maxima of  $n_e$  and  $n_s$  exhibited by references [16] and [17] correspond to the upper limit of the optimum pressure range while that from the present system occur at the lower limit. This discrepancy could be related to the homogeneity of the hollow cathode discharge as the configuration of references [16] & [17] have two anodes, one at each opened end of the cathode while the present system has only one anode at one end.

The ratio of the number of fast to slow electrons  $n_f/n_s$  in the three systems compared manifests minima at  $ap$  close to the upper limit of the respective optimum  $ap$  range. The magnitude of this ratio is lowest in the system of reference [17] (range: 0.14 – 0.05) and highest in reference [16] (range: 23.8 – 0.2). The ratio in the present system is in-between the two ranges above (1.69 – 0.06 at the axis; 0.52 – 0.04 at the side). These magnitudes correspond to the discharge current, whereby, discharge current is the lowest at 20 mA in reference [17], highest at 50 mA in reference [16] and in between at 40 mA in the present system.

**TABLE 1** Summary of the configuration of the various hollow cathode systems compared.

(1)	<b>Present system:</b> Helium gas – stainless steel cathode with one anode HC6512: ratio $\ell:a = 1.85$ HC1612: ratio $\ell:a = 0.75$ Discharge current = 40 mA Optimum $ap$ range: 3 – 6 cm-torr (HC6512)
(2)	<b>Tkachenko &amp; Tyutyunnik [16]</b> Helium gas – nickel cathode with two anodes Diameter $a = 30$ mm; length $\ell = 200$ mm (ratio $\ell:a = 6.7$ ) Discharge current = 50 mA Optimum $ap$ range: 0.6 – 2.4 cm-torr
(3)	<b>Howorka &amp; Pahl [17]</b> Argon gas – ? with two anodes Diameter $a = 20$ mm; length $\ell = 74$ mm (ratio $\ell:a = 3.7$ ) Discharge current = 20 mA Optimum $ap$ range: 0.4 – 0.6 cm-torr

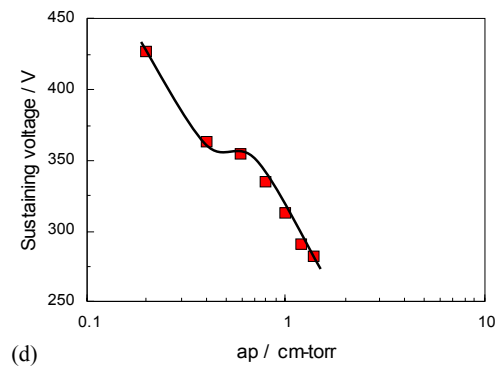
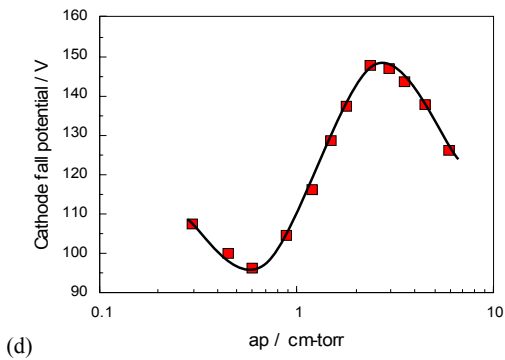
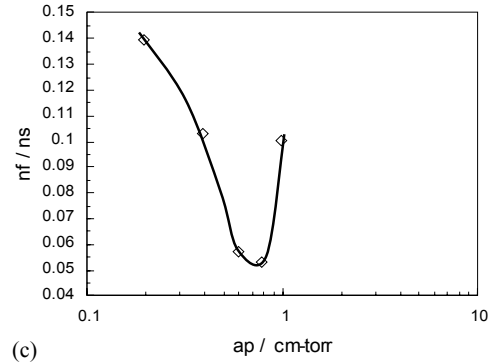
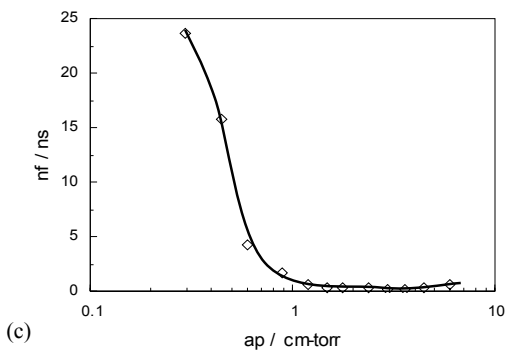
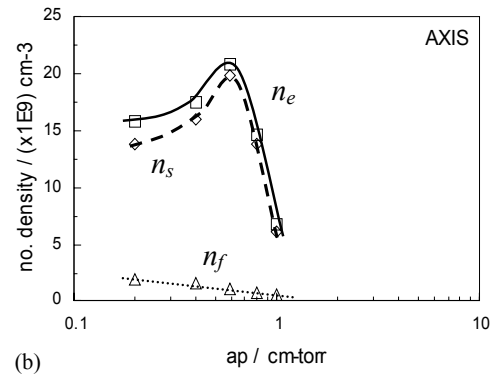
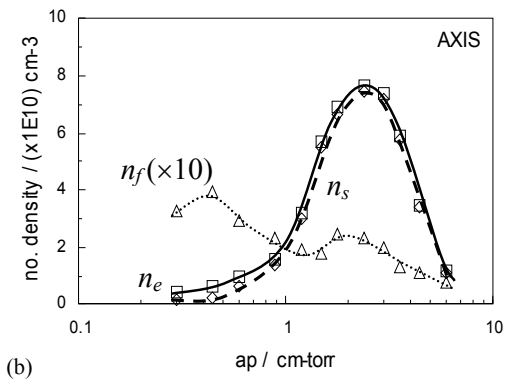
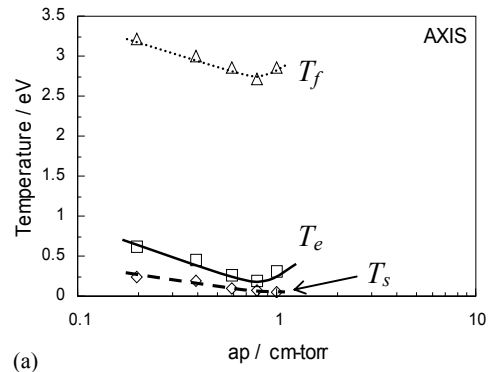
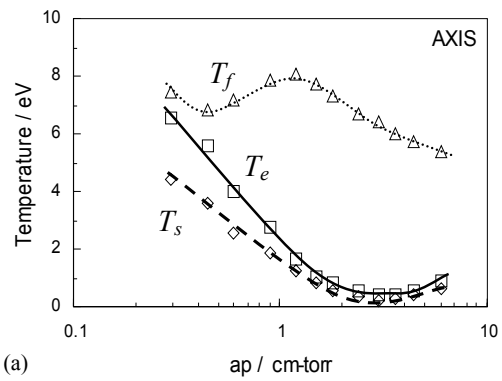


FIG. 9. Dependence of various plasma parameters on the product  $ap$  obtained from reference [16].

FIG. 10. Dependence of the various plasma parameters on the product  $ap$  obtained from reference [17].

#### IV. CONCLUSION

It is concluded that the electron temperatures, electron densities and the ratio of the number of fast to slow electrons in a dc helium hollow cathode discharge can be correlated to the optimum pressure range defined by Kirichenko et al. [7]. The dip in the variation of  $T_e$  and  $n_f/n_s$  with  $ap$  corresponds roughly to the upper limit of this optimum pressure range. The peak in  $n_e$  and  $n_s$  also corresponds to this upper limit for references [16] and [17]; while the same peaks in the present system correspond to the lower limit. This discrepancy is likely to be attributed to the homogeneity of the hollow cathode discharge formed.

#### ACKNOWLEDGEMENT

The authors are grateful to the Ministry of Science, Technology and the Environment of Malaysia for supporting this work under IRPA Program 4-07-04-40-05.

#### REFERENCES

- [1] F. Paschen, *Ann. Phys.*, **50**, 901 (1916).
- [2] J.W. Gewartowski and H.A. Watson, *Principles of electron tubes*, Van Nostrand, Princeton, New Jersey (1965), pp. 56.
- [3] C.S. Willet, *Introduction to gas lasers: population inversion mechanisms*, Pergamon Press, New York (1974), pp.79.
- [4] P.F. Little and A. von Engel, *Proc. Roy. Soc.*, **A224**, 209 (1954).
- [5] D. Ciobotaru, *J. Electron. Control*, **17**, 529 (1964).
- [6] V.S. Borodin and Yu.M. Kagan, *Sov. Phys. – Techn. Phys.*, **11** (1), 131 (1966).
- [7] V.I. Kirichenko, V.M. Tkachenko and V.B. Tyutyunnik, *Sov. Phys. – Techn. Phys.*, **21** (9), 1080 (1976).
- [8] H. Helm, *Z. Naturforsch.*, **27A**, 1812 (1972).
- [9] P. Gill and C.E. Webb, *J. Phys. D: Appl. Phys.*, **10**, 299 (1977).
- [10] E. von Badareu, I. Popescu and I. Iova, *Ann. Phys. – Leipzig*, **5**, 308 (1960).
- [11] D.J. Sturges and H.J. Oskam, *Physica*, **37**, 457 (1967).
- [12] H.L. Witting, *J. Appl. Phys.*, **42**, 5478 (1971).
- [13] A.D. White, *J. Appl. Phys.*, **30** (5), 711 (1959).
- [14] T. Musha, *J. Phys. Soc. Jpn.*, **17**, 1440 (1962).
- [15] G. Francis, *Handbook der physik*, edited by S. Flügge, **22**, Springer-Verlag, Berlin (1956), p..53.
- [16] V.M. Tkachenko and V.B. Tyutyunik, *Sov. Phys. – Tech. Phys.*, **21** (7), 825 (1976).
- [17] F. Howorka and M. Pahl, *Z. Naturforsch.*, **27A**, 1425 (1972).